Innovative driving scheme for electrical generators in more electric aircrafts employing series active filtering

Nena Apostolidou, Nick Papanikolaou
DEMOCRITUS UNIVERSITY OF THRACE
DEPARTMENT OF ELECTRICAL AND COMPUTER ENGINEERING
ELECTRIC MACHINES LABORATORY
ECE Campus, Building B', Office 012
Kimmeria Xanthi, Greece, 67132
Tel.: +30.2541079739, +30.2541079921
E-Mail: paposto@ee.duth.gr, npapanik@ee.duth.gr

Acknowledgements

This research was supported by the Hellenic Foundation for Research and Innovation (HFRI) under the HFRI PhD Fellowship grant (Fellowship Number: 118)

Keywords

«Aerospace», «Switched reluctance drive», «Microgrid», «Generation of electrical energy», «Active filter».

Abstract

As more electrification of the future aircrafts becomes a trend, more electric functions, such as the Starter/Generator (S/G) that are incorporated in the More Electric Aircrafts (MEA) concept, increase the need for electrical power systems with high power supply capabilities, facilitating both motor (starter) and generator operation. Under this light, an innovative driving scheme for electrical generators in MEA that employs series active filtering (SAF) is proposed in this paper, to impose the desired output current in the dc microgrid (DCMG) of the MEA, thus facilitating the multi-operating-point range capability of the machine drive. The proposed SAF-based system that facilitates the incorporation of multiple energy storage units (ESUs) constitutes a robust S/G solution that serves this double-mode operation requirement (set by the specific application), along with the wide set point range necessity of the power generation mode. Moreover, an appropriately developed Design Tool allows for the selection of the optimal SAF parameters, according to the DCMG and the machine drive specifications, facilitating high performance and reliability of the proposed drive unit. The developed S/G driving scheme is verified through MATLAB/Simulink simulations and, additionally, the performance of the power generation control of the system under study is evaluated via real-time control hardware in-the-loop (CHIL) tests, with the use of a dedicated microcontroller (dsPIC30f4011) and dSPACE 1202 (MicroLabBox) platform.

Introduction

The innovative driving scheme deals with the electrical energy production of the electric generators that are incorporated in the MEA [1], under the necessity of the efficient operation of these machines over a wide operating point range, that is imposed by the vast load changes of the MEA power system; under this light, the key-feature of the innovative driving scheme lies in the direct power control over the electrical generator, through the incorporation of a SAF in its control unit, as depicted in Fig. 1(a). In addition, an appropriate vector control scheme is implemented on the SAF (incorporating various ESUs), which is suitable for the S/G drive unit, facilitating both the acceleration of the machine during starting mode (enhancing the machine's starting electromagnetic torque production, T_e) and the efficient power control at various operational points during generator mode.

The developed active power control scheme is extendable, thus applicable to any converter-fed, multi-phase machine (i.e., N_{Ph} number of phases can be considered), which is advantageous in terms of power quality improvement, by mitigating the current/torque pulsation impact at the point of common coupling (PCC); at the same time, the SAF is compatible with any type of electrical machine drive, thus allowing for the incorporation of various types of alternative SAF solutions, comprising of any *n*-level DC/AC converter (*n*, number of levels of the multilevel converter) and various alternative voltage source units (such as capacitors and/or batteries) that are suitable for each machine drive case, as Fig. 1(a) illustrates.

In addition, an appropriately developed Design Tool (Fig. 2) allows for the selection of the optimal SAF parameters (i.e., the Design Tool outputs, according to Fig. 2a), thus constituting a general tool that is totally adaptable to the specifications of any candidate electric drive system (i.e., the Design Tool inputs, according to Fig. 2a) to be integrated in the MEA DCMG, as well as in other similar systems that use electrical machine drives under this frame (which can be modeled in an appropriate dedicated software environment).

Furthermore, the innovative driving scheme allows for the minimization of the electrical variables' real time feedback, while the SAF incorporation inherently serves the fault-ride through capability (FRTC) of the drive system (i.e., in terms of power generation loss avoidance in cases of under/over voltage conditions) and facilitates the incorporation of energy management/storage electric apparatus.

On the other hand, the developed Design Tool facilitates the enhancement of the reliability of the total drive system through the optimum design and integration of electrical apparatus/units of high reliability, such as film capacitors, which can be used in the SAF (replacing the bulky electrolyte capacitors which are used in relevant applications). These features are of outmost importance for the MEA DCMG operation.

In this paper, for the implementation of the proposed SAF-based active power control concept, the switched reluctance machine (SRM) is used as the S/G unit, being among the most attractive candidates to perform the electric starting of the main engine, due to its unique physical characteristics that favor its direct coupling to the propulsive unit. Thus, the design of the system parameters as well as the presented results, i.e., the MATLAB/Simulink simulations (regarding the S/G concept, i.e., motor and generator operation) along with the real-time CHIL tests – verifying the effectiveness of the control scheme implementation on the switched reluctance generator (SRG), are based on the torque production mechanism of the specific machine type (i.e., the SRM's current and torque profile). However, these results verify in an excellent manner the proposed vector-controlled SAF concept (including the circuit topology and the Design Tool), which can be used in various machine drives (with the appropriate adjustment), as well.

The proposed innovate driving scheme along with the developed Design Tool have been patented under the Hellenic Industrial Property Organization (Patent Nr.1010204).

Case study: Implementation of the innovative driving scheme in the SRM

When it comes to the potential MEA electrical generators, the SRM has been recognized as one of the most promising candidates to be incorporated in the energy generation/distribution system of the MEA [2]. In light of this, the innovative driving scheme has been implemented for the control of the generated power of an SRG that is incorporated in the MEA high-voltage DCMG; in this case study, the Design Tool implementation regards the determination of the optimum SAF parameters that facilitate the specific machine's operational features, as it will be presented.

In the relative literature, there are numerous publications regarding the incorporation of the SRG in high power systems, such as those which are used in electrified aircrafts [3], that focus on the control upon the optimal operational point of the machine, either under motor or generator mode, especially for the S/G function [4]; however, these studies do not conclude to a reliable solution that facilitates the MEA multi-operational control feature that is discussed in the Introduction. More specifically, although in

recent literature there are many studies regarding several SRM control schemes [5], [6], these studies do not focus on high power systems, such as the DCMG of the electrified aircraft, where the necessity of multi-operational generated power levels calls for the uninterrupted operation of the SRG under various operational points. What is more, the active front-end converter filtering solutions that have been recently proposed in relative literature [7], [8] (attempting to enhance the output power range and efficiency of the SRG in a wider speed operating range), face specific limitations, which are analyzed in depth in [9].

Under this light, the innovative driving scheme implementation (with the use of the developed Design Tool) in the SRM's case has been verified by both simulations (in MATLAB software environment) and real time implementation, with the use of an appropriate CHIL set-up (dSPACE 1202 platform) along with an external dedicated signal processor (dsPIC30f4011). It is noted that the presented simulation results regarding the S/G concept, that are oriented upon the high-voltage (270V) and high-power MEA application (which present both the steady state operation and the control response under transient conditions, highlighting the FRTC and dispatchability features of the innovative driving scheme), proved that the innovative active power control scheme is capable of enhancing the reliability and reducing the computational burden of the electrified aircrafts' application under study. On the other hand, the real time performance results that are presented in this paper are oriented upon the verification of the effectiveness of the real time control implementation during generator operation, under reduced voltage and speed conditions (resulting from the hardware limitations, as it will be explained).

Description of the Innovative Driving Scheme

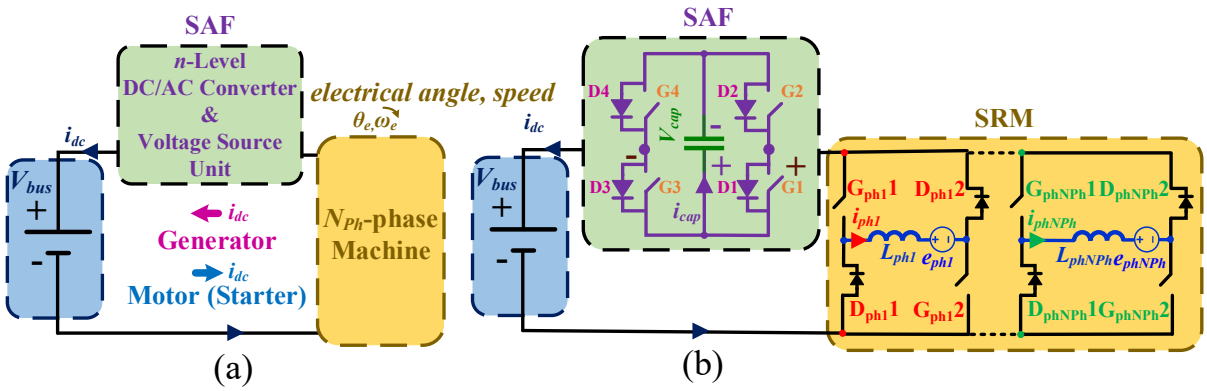

Fig. 1: DCMG voltage, V_{bus}, and instantaneous DCMG current, i_{dc}, (a) general-type machine drive case: SAF with a n-level DC/AC converter and a voltage source unit; N_{Ph}-phase machine (b) SRM drive case: SAF with a single-phase HBC and a capacitive voltage source (average SAF capacitor voltage, V_{cap}); N_{Ph}-phase SRM, with integrated asymmetric H-bridge converter (AHBC) – i_{ph}, e_{ph} and L_{ph} are the phase current, back-electromotive force (BEMF) – voltage – and inductance, respectively.

Regarding Fig. 1, the innovation of the control scheme as far as a N_{Ph}-phase SRM is considered – Fig.1(b), lies on the imposition of the desired SRM's output current (mean value), I_{dc} (in the specific application the reference current regards the high voltage DCMG side, V_{bus}), which is achieved through the independent control of the phases' magnetization current, I_{mag}, and the DCMG current, i_{dc}, with the application of the proper operational states of the switches in a 2-level H-bridge converter – HBC (these states are referred as voltage vectors (v_x), according to Tables I and II) – acting as the SAF.

In generator mode the goal is to provide constant current to the DCMG, thus the vector control is oriented upon i_{dc} feedback signal, according to the following ordinary differential equations (ODEs), corresponding to Fig. 1 (generator mode) and Table I:

$$\left.\frac{di_{dc}}{dt}\right|_{x=1,4,6} = \frac{-v_x - \overbrace{\omega_e \frac{dL_{phNPh}}{d\theta_e} i_{phNPh}}^{e_{phNPh}}}{L_{phNPh}} + \ldots - \frac{v_x - \overbrace{\omega_e \frac{dL_{ph1}}{d\theta_e} i_{ph1}}^{e_{ph1}}}{L_{ph1}}, \quad (1)$$

$$\left.\frac{di_{dc}}{dt}\right|_{x=2,3,5,7} = \frac{-v_x - \overbrace{\omega_e \frac{dL_{ph1}}{d\theta_e} i_{ph1}}^{e_{ph1}}}{L_{ph1}} + \ldots + \frac{-v_x - \overbrace{\omega_e \frac{dL_{phNPh}}{d\theta_e} i_{phNPh}}^{e_{phNPh}}}{L_{phNPh}} \quad (2)$$

The impact of the application of each voltage vector on i_{dc} and v_{cap} (instantaneous SAF capacitor voltage) during generator mode is presented in Table I, regarding the use of a capacitive ESU in the SAF input, which is properly charged and discharged (according to the applied voltage vector), so that it preserves the SAF capacitor voltage level ($V_{cap,ref}$).

Table I: Possible operational States of SAF circuit during generator mode, with capacitive ESU (v_{cap}): (↑) Increase, (↓) Decrease, (==) No change.

Voltage Vector	SAF Active Switch(es), Diode(s)	Generator Mode Active Voltage	i_{dc}	v_{cap}
1/4	G1, D3/G4, D2	$v_{1,4}=V_{bus}$ (Over-magnetization[1])	↓	==
2/3	G2, D4/G3, D1	$v_{2,3}=V_{bus}$ (Generation)	↑	==
5	G2, G3	$v_5=V_{bus}-v_{cap}$ (Generation)	↑	↓
6	G1, G4	$v_6=V_{bus}+v_{cap}$ (Over-magnetization[1])	↓	↓
	D1, D4	$v_6=V_{bus}+v_{cap}$ (Under-magnetization[2])		↑
7	D1, D4	$v_7=V_{bus}+v_{cap}$ (Generation)	↓	↑

[1] $I_{mag}<0$ (with respect to the current flow in Fig. 1, generator mode), over-magnetization [9].
[2] $I_{mag}>0$ (with respect to the current flow in Fig.1, generator mode), under-magnetization [9].

On the other hand, the SAF operation during starter mode is based upon the control of the SRM's phases' currents sum, $i_{Ph}=i_{ph1}+\ldots+i_{phNPh}$, with respect to Fig. 1(b), according to the following ODEs, corresponding to Fig. 1 (motor mode) and Table II:

$$\left.\frac{di_{Ph}}{dt}\right|_{x=1\div7} = \frac{v_x - \overbrace{\omega_e \frac{dL_{ph1}}{d\theta_e} i_{ph1}}^{e_{ph1}}}{L_{ph1}} + \ldots + \frac{v_x - \overbrace{\omega_e \frac{dL_{phNPh}}{d\theta_e} i_{phNPh}}^{e_{phNPh}}}{L_{phNPh}} \quad (3)$$

$$\left.\frac{di_{Ph}}{dt}\right|_{x=1\div7} = \frac{v_x - \overbrace{\omega_e \frac{dL_{ph1}}{d\theta_e} i_{ph1}}^{e_{ph1}}}{L_{ph1}} + \ldots + \frac{-v_x - \overbrace{\omega_e \frac{dL_{phNPh}}{d\theta_e} i_{phNPh}}^{e_{phNPh}}}{L_{phNPh}} \quad (4)$$

Table II presents the voltage vectors that are used in the motor (starter) mode, with the incorporation of a various type ESU (implemented as a constant voltage source, V_{ESU}), providing the necessary power to the SRM for the starting torque production.

The proposed control scheme is general/adaptable in various conditions/parameters of the system, such as the speed, the amounts of the produced energy/power, current and voltage level restrictions (nominal values of the SRM, the SAF and the DCMG) and load conditions (which determine the over/under magnetization operation of the SRG), resulting in the capability of the machine drive in a wide operating point range (dispatchability feature), as well as in a smooth transition from generator to motor operation and vice versa, under any speed. In any case, the power flow control is implemented without the need for real time processing of the electrical machine parameters (the machine's power control is

independent from the conventional angle power control of the SRMs), which leads to the reduction of the computational burden of the control system and enhances the total reliability of the system.

Table II: Possible operational States of SAF circuit during motor mode, with any type ESU (constant voltage source, V_{ESU}): (↑) Increase, (↓) Decrease, (==) No change.

Voltage Vector	SAF Active Switch(es), Diode(s)	Motor Mode Active Voltage	i_{Ph}	ESU
1/4	G1, D3/G4, D2	$v_{1,4}=V_{bus}$	↑/↓ [2]	==
2/3	- [1]	$v_{2,3}=0$	↑	==
5	G2, G3	$v_5=V_{bus}-V_{ESU}$	↑ [3]	**discharge**
6	G1, G4	$v_6=V_{bus}+V_{ESU}$	↑	**discharge**
7	- [1]	$v_7=0$	↓	==

[1] i_{ph} flows through G_{ph} and D_{ph} in Fig. 1(b) [9].
[2] dictated by BEMF's magnitude, which is proportional to ω_e and the phase current [9].
[3] refers only to the phases' commutation interval [9].

Development of the SAF Design Tool

The developed Design Tool of the proposed SAF – general case, Fig. 2(a) – facilitates the adaptation of the control design to the requirements of the system/microgrid under study – general case, Fig. 2(a) – and the characteristics of the incorporated machine type. In the SRG case under study (the analytical description of the control scheme is given in [9]), the selection of the optimal values of the total system's parameters of the circuitry of Fig. 1(b) is based upon the system's specifications/restrictions which regard the maximum produced power level ($I_{dc,max}$), the maximum SAF capacitor voltage level ($V_{cap,max}$), the maximum SAF capacitor voltage deviation ($\Delta V_{cap,max}$) and the maximum SAF switching losses ($P_{sw,loss,,max}$); these values are the inputs of the Design Tool and, with the implementation of the appropriate control algorithm that interacts with the developed simulation model – Fig. 2(b), they determine the outputs of the Design Tool (the analytical description of the developed Design Tool is given in [9]); in the present SRG case study, where a capacitive ESU is considered and the hysteresis current control is implemented, the outputs of the Design Tool regard the maximum i_{dc} reference value ($I_{ref,max}$) that is used for the SRG's control implementation pattern, as well as the optimal parameters of the SAF, regarding the minimum capacitance value C_{min} (so that film capacitors can be used) and the minimum hysteresis zone (H_{min}), so that good i_{dc} profile (more constant) is achieved. Under this frame, the system is designed upon the maximum operating point (MOP), which is defined as MOP($I_{dc,max}$ (A), $V_{cap,max}$ (V)).

The advantages of the innovative active power control scheme regarding the SRM case study are summarized in the following features:

- Robust driving of the machine in the double-mode operation of the S/G application; reliable starting/acceleration of the SRM and smooth transition from motor to generator mode, though the implementation of the same control pattern (SAF vector control).
- Controllability over a wide operating point range for the electrical energy production, in generator mode. This is achieved through the independent control of I_{mag} and i_{dc}, thanks to the integration of the SAF; the magnetization current control also facilitates the control/definition of the desired/acceptable SAF capacitor voltage level ($V_{cap,ref}$).
- Limitation of the switching frequency of the SRM's phases converter (AHBC) to the basic electrical frequency (out of the SRM's rotational speed, RPM), which is a requirement for the production of high energy amounts, with high efficiency (limitation of the AHBC's switching losses).
- Capability of integrating an appropriate electrical unit for the energy management and storage, with the use of highly reliable electrical apparatus (e.g., film capacitors).
- High reliability of the machine under both stand-alone and dc-microgrid connected operation (e.g., aircrafts' systems).

- Elimination of additional passive elements, such as inductors and capacitors, which reduce the reliability and the gravimetric/volumetric power density of the system.
- Low complexity of the control scheme; the AHBC operates only in two basic modes (that is the phases' magnetization when the switches are on and the phases' generation through the free-wheeling diodes), while the total control scheme is implemented by the SAF.
- Inherent FRTC; during impermanent faulty conditions (e.g., DCMG voltage overshoots/dips), the SAF facilitates the uninterruptable SRM's energy production.

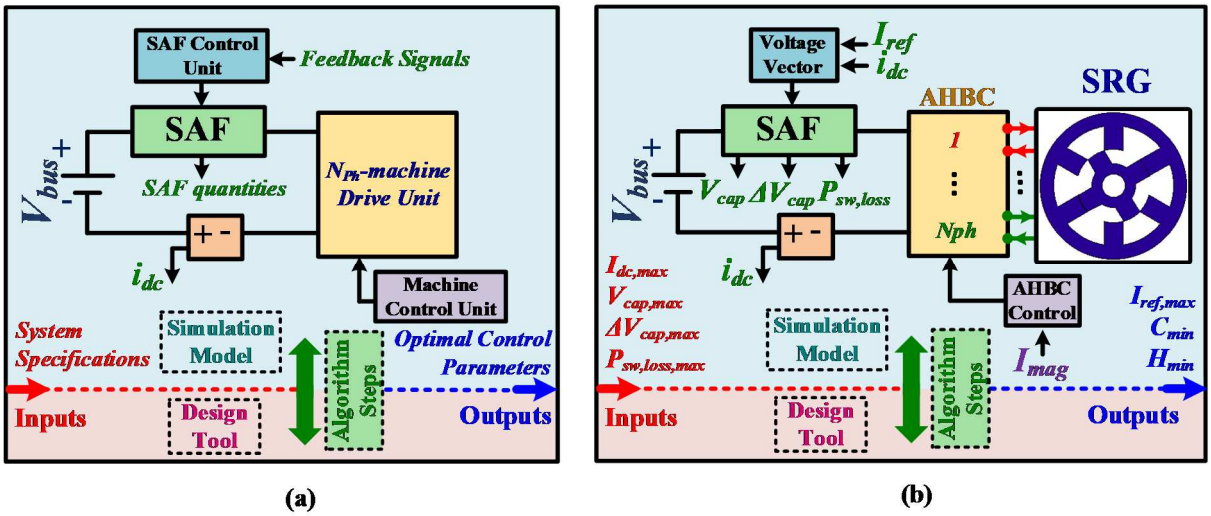

Fig. 2: Design Tool for the selection of the optimal values of the total system's parameters; (a) General electrical machine drive system and SAF, according to Fig. 1(a), (b) SAF and SRG drive system according to Fig. 1(b).

CHIL Verification results regarding the generator operation

The real-time performance of the developed control scheme in the 6/4, 3-phase SRG case study [9] has been verified through an appropriate CHIL set-up – Fig. 3(d), comprising of a dSPACE MicroLabBox 1202 platform (combined with MatlabR2014b software), running at a 10 kHz sampling frequency, in cooperation with an external microcontroller hardware, i.e., the dsPIC30f4011 DSP, running at 7.37 MHz; more specifically, dsPIC30f4011 receives real time feedback signals (as inputs) from the simulation model which is built in MicroLabBox 1202, implements the proposed control algorithm and sends the appropriate AHBC and SAF control signals (as outputs) back into MicroLabBox 1202. dSPACE Control Desk software performs data acquisition and visualization of the real time signals. It is noted that due to the MicroLabBox 1202 hardware limitation of 10 kHz real time simulation, the SRM model is evaluated to the limit of RPM=800 rpm and V_{bus}=48 V.

Fig. 3(a) and (b) present the CHIL implementation results regarding the real time response of the control (through the appropriate response of I_{mag}), under step changes of i_{dc} reference value, I_{ref}. In Fig. 3(a), I_{mag} is decreased from -49.1 A to -50.7 A when I_{ref} is increased from 60 A to 125 A (at 4 s time spot), while I_{mag} is further decreased from -50.7 A to -74.3 A when I_{ref} is further increased from 125 A to 200 A (at 24 s time spot). In any case, the SAF capacitor charges and discharges (according to the pattern of Table I) to preserve the reference voltage value, $V_{cap,ref}$, which in this case has been selected to 48V.

Fig. 3(c) illustrates the response of the control scheme under a V_{bus} drop, from 48 V to 0 V, from 3.525 s until 3.672 s time spot (the 147 ms abnormal voltage drop duration complies with MIL-STD-704F disturbances limits). During this interval, the SAF capacitor absorbs the SRG's energy, highlighting the FRTC capability of the developed control scheme under real time implementation.

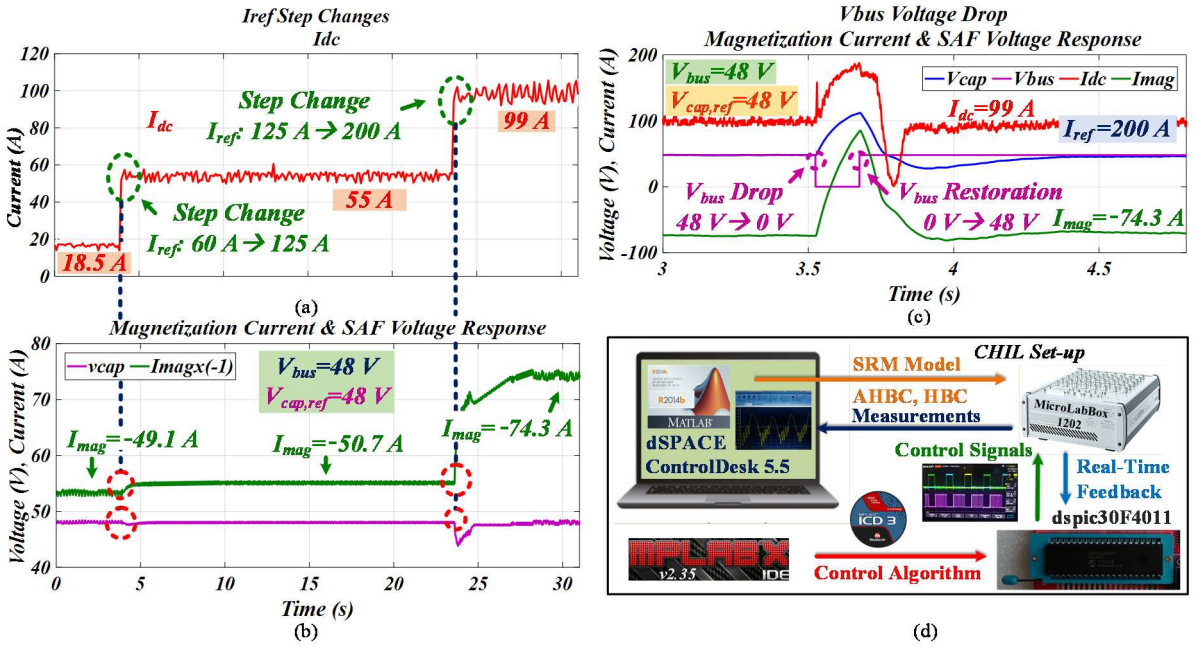

Fig. 3: (a), (b) i_{dc}, I_{mag} (the sign of I_{mag} is according to the current flow of Fig. 1, generator mode) and v_{cap} response, under I_{ref} step changes, from 60 A to 125 A at 4 s time spot and from 125 A to 200 A at 24 s time spot, (c) I_{mag} and V_{cap} response, under V_{bus} voltage drop at 3.525 s time spot, MOP(100 A, 48 V), V_{bus} restoration at 3.672 s time spot, (d) Block diagram of the CHIL set-up for the real time validation of the proposed control scheme [9].

MATLAB simulation results regarding the S/G concept

The performance of the developed S/G control scheme (regarding the 6/4, 3-phase SRG case study [9] of the CHIL tests) is modeled in MATLAB R2018b software, according to the circuitry of Fig. 1(b) and 2(b), as depicted in the results depicted in Fig. 4.

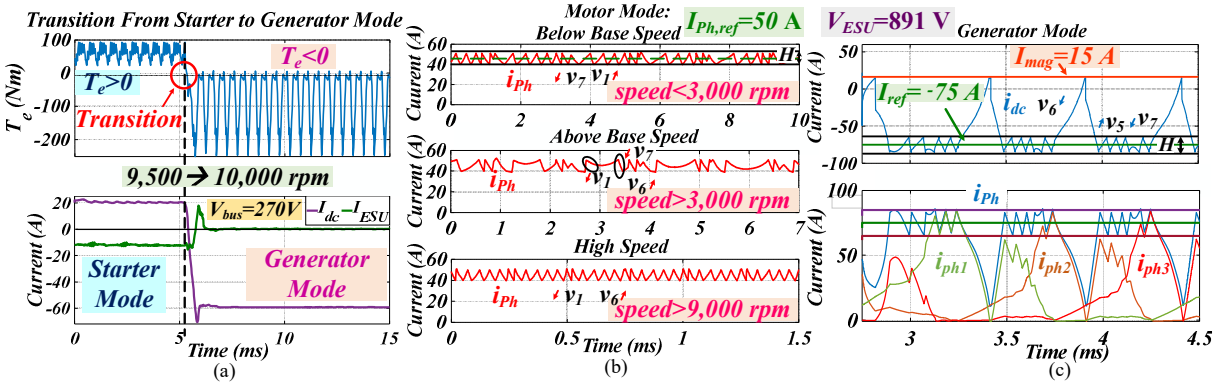

Fig. 4: (a) Transition from starter mode (T_e, I_{dc}, i_{dc}>0, with respect to the direction of the current flow in motor mode in Fig. 1) to generator mode (T_e, I_{dc}, i_{dc}<0, with respect to the direction of the current flow in motor mode in Fig. 1), generator , (b) vector control implementation during starter mode (Table II), under i_{Ph} reference value, $I_{Ph,ref}$=50 A and V_{ESU}=891 V, below/above base speed and at high speed, (c) vector control implementation during generator mode (according to Table I, where v_{cap}=V_{ESU}), with I_{ref}=-75 A (i_{dc}<0, with respect to Fig. 1, motor mode) and V_{ESU}=891 V – i_{ph1}, i_{ph2}, i_{ph3} are the phase currents.

The SRM predetermined model (incorporating a detailed mapping over the SRM technical characteristics based on FEA) that is used in the developed simulation model, along with the SAF control implementation parameters have been selected with the use of the developed Design Tool, which has been presented in [9], allowing for the determination of the optimum energy balance point (EBP) of the system under study (Fig. 1 and 2). The EBP refers to the condition that the ESU neither provides nor

absorbs energy during a control pattern implementation period (regarding the generator operation), thus the average ESU current, I_{ESU}, is zero.

Fig. 4(a) verifies the successful transition of the SRM from starter to generator mode (with the aid of the vector control of Tables I and II); during starter mode (I_{dc}>0) the ESU provides energy to the SRM (average current of the ESU, I_{ESU}>0), while during generator mode (I_{dc}<0) the EBP (I_{dc}=-60A) is reached (I_{ESU}=0). Furthermore, Fig. 4(b) illustrates the vector control implementation during motor (starter) mode, accelerating the SRM from standstill to the speed that the machine enters the generator mode (in this case 10,000 rpm [9]); the latter mode of operation is depicted in Fig. 4(c), which regards the power generation (i_{dc}<0, with respect to Fig. 1, motor mode) at I_{ref}=-75A and I_{mag}=15A (over-magnetization).

Conclusion

The innovative driving scheme facilitates the direct power control of the electrical generators, through the imposition of the desired machine's output current value, thus facilitating the capability of the multi-operating point range machine mode, in line with the dispatchability requirements of MEA electric power systems. In addition, the incorporation of an ESU in the SAF circuitry facilitates the reliable starting torque production during motor (starter) mode of the S/G application; the developed Design Tool facilitates the adaptability of the power control scheme implementation under various specifications and restrictions of the system under study. The innovative control scheme has been verified via the developed simulation models both in software and in real time processing hardware.

References

[1] W. Cao, B. C. Mecrow, G. J. Atkinson, J. W. Bennett, and D. J. Atkinson, "Overview of electric motor technologies used for more electric aircraft (MEA)," IEEE Trans. Ind. Electron., vol. 59, no. 9, pp. 3523–3531, Sept. 2012.

[2] V. Madonna, P. Giangrande and M. Galea, "Electrical power generation in aircraft: review, challenges, and opportunities," IEEE Trans. Transp. Electrif., vol. 4, no. 3, pp. 646–659, Sept. 2018.

[3] S. Li, S. Zhang, T. G. Habetler, and R. G. Harley, "Modeling, design optimization and applications of switched reluctance machines – a review," IEEE Trans. Ind. Appl., vol. 55, no. 3, pp. 2660–2681, May/Jun. 2019.

[4] J. K. Nøland, M. Leandro, J. A. Suul, and M. Molinas, "High-power machines and starter-generator topologies for more electric aircraft: a technology outlook, IEEE access, vol. 8, pp. 130104–130123, Jul. 2020.

[5] S. Song, R. Hei, R. Ma and, W. Liu, "Model predictive control of switched reluctance starter/generator with torque sharing and compensation," IEEE Trans. Transp. Electrif., vol. 6, no. 4, pp. 1519–1527, Dec. 2020.

[6] R. Rocca, F. G. Capponi, S. Papadopoulos, G. D. Donato, M. Rashed, and M. Galea, "Optimal advance angle for aided maximum-speed-node design of switched reluctance machines," IEEE Trans. Energy Conv., vol 35, no. 2, pp. 775–785, Jun. 2020.

[7] A. Klein-Hessling, B. Burkhart and R. W. De Doncker, "Active source current filtering to minimize the DC-link capacitor in switched reluctance drives," IEEE Trans. Power Electron. Appl., vol. 4, no. 1, pp. 62–71, Mar. 2019.

[8] Q. Wang, H. Chen, H. Cheng, S. Yan and S. Abbas, "An active boost power converter for improving the performance of switched reluctance generators in dc generating systems," IEEE Trans. Power Electron., vol. 35, no. 5, pp. 4741–4754, May 2020.

[9] N. Apostolidou and N. Papanikolaou, "Active Power Control of Switched Reluctance Generator in More Electric Aircraft," IEEE Trans. Veh. Techn., Vol. 70, Issue 12, pp. 12604-12616, Dec. 2021.